Computers and Mathematics with Applications 63 (2012) 794–806

Contents lists available at SciVerse ScienceDirect

Computers and Mathematics with Applications

journal homepage: www.elsevier.com/locate/camwa

A new preconditioner for the interface system arising in a fast Helmholtz solver

Kui Du *

School of Mathematical Sciences, Xiamen University, Xiamen 361005, China

ARTICLE INFO

Article history:
Received 4 May 2011
Received in revised form 22 November 2011
Accepted 22 November 2011

Keywords:
Electromagnetic scattering
Helmholtz equation
Nonlocal boundary condition
Optimal sine transform based approximation
Layered medium
Preconditioning

ABSTRACT

In this paper, on the basis of the optimal sine transform based approximation we propose a new preconditioner for the interface system arising in the fast Helmholtz solver [G. Bao, W. Sun, A fast algorithm for the electromagnetic scattering from a large cavity, SIAM J. Sci. Comput. 27 (2005) 553–574 (electronic)] for the electromagnetic scattering from a large cavity with layered media. We show that the spectrum of the preconditioned matrix is clustered around 1 if the preconditioner is not nearly singular. Numerical results show that the number of iterations of an preconditioned iterative method for the interface system is independent of the mesh size and the wavenumber. The computational cost of the fast method proposed in this paper for calculating the radar cross section, which is very important in electromagnetism, by means of fast Fourier transforms, is $\mathcal{O}(N^2)$ on an $N \times N$ uniform partition of the unit square for the source free case.

1. Introduction

Accurate calculation of the radar cross section (RCS) is a very important subject in electromagnetism. Due to the dominance to the target's overall RCS, electromagnetic scattering from large cavities has attracted much attention recently; see, for example, [1–7] and the references therein. We refer the reader to [8] for a detailed discussion concerning large cavities and related topics.

A fast algorithm was presented in [8] for obtaining the electromagnetic scattering from a large rectangular open cavity in which the medium is vertically layered. On the basis of the use of a discrete Fourier transform in the horizontal direction and a Gaussian elimination in the vertical direction, the algorithm reduces the global system to an interface system on the aperture. This step is equivalent to constructing a discrete Dirichlet-to-Neumann map. The interface system is solved by an iterative method. A simple diagonal preconditioning was used there. Using the fast Fourier transform (FFT) [9], the computational complexity of the fast algorithm is $\mathcal{O}(N^2 \log N) + \mathcal{O}(pN \log N)$ on an $N \times N$ uniform mesh, where p is the number of iterations required by the iterative method for the interface system. For the source free case, the computational cost reduces to $\mathcal{O}(N^2)$ if $p \leq N/\log N$, which was illustrated numerically. Numerical examples show that p is almost independent of the mesh size and increases as the wavenumber increases.

In this paper, on the basis of the optimal sine transform based approximation [10], we proposed a new preconditioner for the interface system arising in the fast algorithm [8]. We show that the spectrum of the preconditioned matrix is clustered around 1 if the preconditioner is not nearly singular. Numerical results show that the number of iterations of the preconditioned conjugate orthogonal conjugate gradient (COCG) method [11,12] (see [13, Chapter 7] for details) is independent of the mesh size and the wavenumber. Therefore, the computational complexity of the resulting fast algorithm is $\mathcal{O}(N^2 \log N)$ on an $N \times N$ uniform mesh and reduces to $\mathcal{O}(N^2)$ for the source free case.

* Correspondence to: Institute of Mathematics, Aalto University, P.O.Box 11100, FI-00076 Aalto, Finland.
E-mail address: kuidumath@yahoo.com.

0898-1221/$ – see front matter
doi:10.1016/j.camwa.2011.11.045

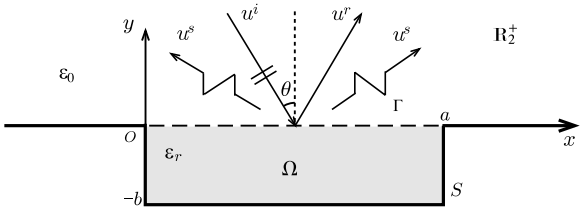

Fig. 1. The cavity geometry.

The rest of this paper is organized as follows. In Section 2, we introduce the cavity problem. We present the framework of the fast algorithm and the new preconditioner in Section 3. The spectrum of the preconditioned matrix of the interface system is analyzed in Section 4. We report the numerical results for a model problem in Section 5. We present brief concluding remarks on this work in Section 6.

2. Electromagnetic scattering from a large cavity

We consider the electromagnetic scattering from a cavity embedded in the ground plane [4]; see Fig. 1. Assume that the medium and the material are invariant in the z-direction. Assume also that the medium is non-magnetic and a constant magnetic permeability $\mu(x, y) = \mu_0$ exists everywhere. The half-space above the ground plane is filled with a homogeneous, linear, isotropic medium with the electric permittivity ε_0. The electromagnetic property of the medium is characterized by the relative permittivity $\varepsilon_r(x, y) = \varepsilon(x, y)/\varepsilon_0$. For simplicity, we only consider the real and positive medium case, i.e., $\varepsilon_r > 0$.

For the transverse magnetic (TM) polarization, in which the magnetic field is transverse to the invariant direction and the electric field E has the form $(0, 0, u(x, y))$, the time-harmonic Maxwell equations reduce to the Helmholtz equation together with Sommerfeld's radiation condition imposed at infinity,

$$\begin{cases} \Delta u + k_0^2 \varepsilon_r u = f & \text{in } \Omega \cup R_2^+, \\ u = 0 & \text{on } \partial(\Omega \cup R_2^+), \\ \lim\limits_{r\to\infty} \sqrt{r}(\partial_r u^s - \mathrm{i}k_0 u^s) = 0 & \text{at } \infty, \end{cases} \tag{2.1}$$

where the free space wavenumber $k_0 = \omega\sqrt{\varepsilon_0\mu_0}$, $\Omega = [0, a] \times [-b, 0]$, R_2^+ denotes the upper half-plane, f is the source term and $f = 0$ in R_2^+, $r = \sqrt{x^2 + y^2}$, u^s is the scattered field and $\mathrm{i} = \sqrt{-1}$ is the imaginary unit.

Assume that a plane wave $u^i = e^{\mathrm{i}(\alpha x - \beta y)}$ is incident on the cavity from the above, where $\alpha = k_0 \sin\theta$, $\beta = k_0 \cos\theta$, and $-\pi/2 < \theta < \pi/2$ is the incident angle with respect to the positive y-axis. The total fields consist of three parts: incident (u^i), reflected (u^r) and scattered (u^s) fields. Therefore, the scattered field can be expressed by $u^s = u - u^i - u^r$, where $u^r = -e^{\mathrm{i}(\alpha x + \beta y)}$. Since the upper half-space is homogeneous for the cavity problem, a so-called transparent (nonlocal) boundary condition can be obtained by using the Green's function method [4] or the method of Fourier transforms [14]. Define the nonlocal boundary operator $\mathcal{T}$ as

$$\mathcal{T}(u) = -\frac{k_0}{2} \Xint-_0^a \frac{Y_1(k_0|x-t|)}{|x-t|} u(t, 0)dt + \frac{\mathrm{i}k_0}{2} \int_0^a \frac{J_1(k_0|x-t|)}{|x-t|} u(t, 0)dt, \quad x \in (0, a),$$

where $J_\nu(z)$ and $Y_\nu(z)$ are the Bessel functions [15], and the first term in the right hand side denotes a Hadamard principle value (or finite part) integral [16]. The scattering problem (2.1) is reduced to the following bounded domain problem:

$$\begin{cases} \Delta u + k_0^2 \varepsilon_r u = f & \text{in } \Omega, \quad \text{(a)} \\ u = 0 & \text{on } S, \quad \text{(b)} \\ \partial_n u = \mathcal{T}(u) + g & \text{on}, \quad \text{(c)} \end{cases} \tag{2.2}$$

where S denotes the walls of the cavity, Γ the aperture, ∂_n the normal derivative and $g(x) = -2\mathrm{i}\beta e^{\mathrm{i}\alpha x}$.

3. The fast algorithm

In this section, we review the framework of the fast algorithm proposed in [8] for the cavity problem with vertically layered media and propose a new preconditioner for the interface system arising in the fast algorithm.

Let

$$\Omega_h = \{(x_i, y_j) : i = 0, 1, \ldots, M+1;\ j = 0, 1, \ldots, N+1\}$$

define a uniform partition of $\Omega = [0, a] \times [-b, 0]$ with

$$h_x = \frac{a}{M+1}, \qquad x_i = ih_x, \qquad h_y = \frac{b}{N+1}, \qquad y_j = -b + jh_y.$$

Let u_{ij} be the finite difference solution at the point (x_i, y_j) and $f_{ij} = f(x_i, y_j)$. The discrete finite difference system for (2.2)(a) is given by

$$\frac{u_{i-1,j} - 2u_{ij} + u_{i+1,j}}{h_x^2} + \frac{u_{i,j-1} - 2u_{ij} + u_{i,j+1}}{h_y^2} + k_0^2 \varepsilon_r(y_j) u_{ij} = f_{ij} \tag{3.1}$$

for $i = 1, 2, \ldots, M, j = 1, 2, \ldots, N$. By (2.2)(b), we have

$$u_{0j} = u_{M+1,j} = u_{i0} = 0, \quad i = 1, 2, \ldots, M,\ j = 1, 2, \ldots, N+1.$$

We have, in matrix form,

$$(A_x \otimes I_N + I_M \otimes A_y + I_M \otimes D) u_\Omega + (I_M \otimes a_{N+1}) u_{N+1} = f_\Omega, \tag{3.2}$$

where $\otimes$ denotes the Kronecker product, I_M is the $M \times M$ identity matrix, and

$$\begin{aligned}
&A_x = h_x^{-2} \cdot \text{tridiag}[1, -2, 1],\\
&A_y = h_y^{-2} \cdot \text{tridiag}[1, -2, 1],\\
&D = k_0^2 \cdot \text{diag}\left[\varepsilon_r(y_1), \varepsilon_r(y_2), \ldots, \varepsilon_r(y_N)\right],\\
&a_{N+1} = h_y^{-2}[0, \ldots, 0, 1]^{\mathrm{T}},\\
&u_\Omega = [u_{11}, \ldots, u_{1N}, u_{21}, \ldots, u_{2N}, \ldots, u_{M1}, \ldots, u_{MN}]^{\mathrm{T}},\\
&f_\Omega = [f_{11}, \ldots, f_{1N}, f_{21}, \ldots, f_{2N}, \ldots, f_{M1}, \ldots, f_{MN}]^{\mathrm{T}}.
\end{aligned}$$

By the Toeplitz type approximations in [16, Algorithm II] and the classical trapezoidal rule, the discrete form of the nonlocal boundary condition (2.2)(c) is given by

$$\frac{u_{i,N+1} - u_{iN}}{h_y} = \sum_{j=1}^{M} g_{ij} u_{j,N+1} + g(x_i), \quad i = 1, 2, \ldots, M,$$

where

$$\begin{aligned}
&g_{ij} = g_{ij}^{\mathrm{re}} + \mathrm{i} g_{ij}^{\mathrm{im}},\\
&g_{ij}^{\mathrm{re}} = -t_{ij} \frac{k_0 |x_i - x_j|}{2} Y_1(k_0 |x_i - x_j|),\\
&g_{ij}^{\mathrm{im}} = \frac{k_0 h_x}{2} \frac{J_1(k_0 |x_i - x_j|)}{|x_i - x_j|},
\end{aligned}$$

and

$$t_{ij} = \begin{cases} \dfrac{1}{h_x}(1 - \ln 2), & |i - j| = 1,\\ -\dfrac{2}{h_x}, & i = j,\\ \dfrac{1}{h_x} \ln \dfrac{|i-j|^2}{|i-j|^2 - 1}, & \text{otherwise.} \end{cases}$$

We have, in matrix form,

$$(I_M - h_y G) u_{N+1} - u_N = h_y g, \tag{3.3}$$

where

$$G = (g_{ij})_{i,j=1}^{M}, \qquad u_i = [u_{1i}, u_{2i}, \ldots, u_{Mi}]^{\mathrm{T}},$$

and

$$g = [g_1, g_2, \ldots, g_M]^{\mathrm{T}}, \qquad g_i = g(x_i).$$

By the discrete sine transformation (see Appendix A), we rewrite the discrete linear system (3.2) as

$$(\Lambda \otimes I_N + I_M \otimes A_y + I_M \otimes D) \tilde{u}_\Omega + (I_M \otimes a_{N+1}) \tilde{u}_{N+1} = \tilde{f}_\Omega, \tag{3.4}$$

where

$$\Lambda = \mathrm{diag}\,[\lambda_1, \lambda_2, \ldots, \lambda_M] = S_M A_x S_M,$$
$$\lambda_i = -\frac{4}{h_x^2}\sin^2\frac{i\pi}{2(M+1)},$$
$$\tilde{u}_\Omega = [\tilde{u}_{11}, \ldots, \tilde{u}_{1N}, \tilde{u}_{21}, \ldots, \tilde{u}_{2N}, \ldots, \tilde{u}_{M1}, \ldots, \tilde{u}_{MN}]^{\mathrm{T}} = (S_M \otimes I_N)u_\Omega,$$
$$\tilde{u}_i = [\tilde{u}_{1i}, \tilde{u}_{2i}, \ldots, \tilde{u}_{Mi}]^{\mathrm{T}} = S_M u_i,$$
$$\tilde{f}_\Omega = [\tilde{f}_{11}, \ldots, \tilde{f}_{1N}, \tilde{f}_{21}, \ldots, \tilde{f}_{2N}, \ldots, \tilde{f}_{M1}, \ldots, \tilde{f}_{MN}]^{\mathrm{T}} = (S_M \otimes I_N)f_\Omega.$$

Similarly, (3.3) becomes

$$(I_M - h_y S_M G S_M)\tilde{u}_{N+1} - \tilde{u}_N = h_y \tilde{g}, \tag{3.5}$$

where

$$\tilde{g} = [\tilde{g}_1, \tilde{g}_2, \ldots, \tilde{g}_M]^{\mathrm{T}} = S_M g.$$

Reordering the unknowns and equations in (3.4), we obtain

$$(A_y + \lambda_i I_N + D)\hat{u}_i + a_{N+1}\tilde{u}_{i,N+1} = \hat{f}_i, \quad i = 1, 2, \ldots, M, \tag{3.6}$$

where

$$\hat{u}_i = \left[\tilde{u}_{i1}, \tilde{u}_{i2}, \ldots, \tilde{u}_{iN}\right]^{\mathrm{T}},$$

and

$$\hat{f}_i = \left[\tilde{f}_{i1}, \tilde{f}_{i2}, \ldots, \tilde{f}_{iN}\right]^{\mathrm{T}}.$$

We use the Gaussian elimination method with row partial pivoting to solve the system (3.6). Let

$$A_y + \lambda_i I_N + D = L_i U_i, \quad i = 1, 2, \ldots, M,$$

be the LU factorization, where

$$U_i = (r_{pq}^i).$$

Obviously, L_i is nonsingular. We have, therefore,

$$U_i\hat{u}_i + L_i^{-1}a_{N+1}\tilde{u}_{i,N+1} = \check{f}_i, \quad i = 1, 2, \ldots, M, \tag{3.7}$$

where

$$\check{f}_i = \left[\check{f}_{i1}, \ldots, \check{f}_{iN}\right]^{\mathrm{T}} = L_i^{-1}\hat{f}_i.$$

If the matrix $A_y + \lambda_i I_N + D$ is nonsingular,

$$r_{NN}^i \neq 0, \quad i = 1, 2, \ldots, M.$$

Let $r_{N,N+1}^i$ denote the last component of $L_i^{-1}a_{N+1}$. By the last equations of the systems (3.7)

$$r_{NN}^i\tilde{u}_{iN} + r_{N,N+1}^i\tilde{u}_{i,N+1} = \check{f}_{iN}, \quad i = 1, 2, \ldots, M,$$

and Eq. (3.5), we have

$$(I_M - h_y S_M G S_M + E)\tilde{u}_{N+1} = \check{g}, \tag{3.8}$$

where

$$E = \mathrm{diag}\left[r_{N,N+1}^1/r_{NN}^1, \ldots, r_{N,N+1}^M/r_{NN}^M\right],$$

and

$$\check{g} = \left[\check{f}_{1N}/r_{NN}^1, \ldots, \check{f}_{MN}/r_{NN}^M\right]^{\mathrm{T}} + h_y\tilde{g}.$$

Solving the linear system (3.8) gives the solution $\tilde{u}_{N+1}$ on the interface Γ. The rest of the unknowns can be obtained by solving the system (3.6). If the matrix $A_y + \lambda_i I_N + D$ is singular (or nearly singular) for some $i \in J_s$, where J_s is a subset of $1, 2, \ldots, M$, a special treatment is given; see [8] for details. In all of our numerical tests, J_s is empty, i.e., it suffices to solve the system (3.8).

We obtain the following fast algorithm.

Algorithm I: fast method for electromagnetic cavity problems, TM case	
(i)	Generate the matrix G
(ii)	Calculate $\tilde{f}_\Omega = (S_M \otimes I_N) f_\Omega$ and $\tilde{g} = S_M g$
(iii)	Calculate the LU factorization with row partial pivoting to get U_i, E and $\check{g}$
(iv)	Solve the interface system (3.8) for $\tilde{u}_{N+1}$
(v)	Solve the system (3.6) for $\tilde{u}_\Omega$
(vi)	Calculate $u_\Omega = (S_M \otimes I_N)\tilde{u}_\Omega$ and $u_{N+1} = S_M \tilde{u}_{N+1}$

The key to Algorithm I is how to solve the interface system (3.8) with the coefficient matrix

$$\mathbf{A} = I_M - h_y S_M G S_M + E.$$

Since G is a complex symmetric Toeplitz matrix, the product of the coefficient matrix and a complex vector can be taken in terms of the FFT. We can use a preconditioned iterative solver, such as preconditioned COCG (P-COCG) [11–13] (see Appendix B below for details), for the system (3.8). In [8], the diagonal matrix

$$\mathbf{P} = I_M - \mathrm{i} h_y d_{\mathrm{im}} I_M + E \tag{3.9}$$

was used as a preconditioner, where d_{im} is the diagonal entry of the imaginary part $\Im(G)$ of G. In this paper, on the basis of the analysis in Section 4, we use the following diagonal matrix:

$$\mathbf{M} = I_M - h_y \Lambda_s + E, \tag{3.10}$$

as a preconditioner, where $\Lambda_s = S_M s(G) S_M$ and $s(G)$ is the optimal sine transform based approximation to G (see Appendix A). We refer the reader to [17,18,10,19–21] for more detailed discussion for sine transform based approximation. We remark that in the literature only real symmetric Toeplitz matrices were considered. The extension to the complex symmetric cases is straightforward when considering the real and imaginary parts separately. Our numerical results in Section 5 show that the number of iterations of P-COCG combined with the preconditioner $\mathbf{M}$ is independent of the mesh size and the wavenumber. Therefore, the computational complexity of Algorithm I is $\mathcal{O}(MN \log M)$ when $f \neq 0$ in (2.2)(a); see [8] for details. In the source free case, i.e., $f = 0$, the cost reduces to $\mathcal{O}(MN)$ because only the solution u_{N+1} on the aperture is required for the RCS calculation.

4. The spectrum of the preconditioned matrix $\mathbf{AM}^{-1}$

In this section, we show that the spectrum of the preconditioned matrix $\mathbf{AM}^{-1}$ is clustered around 1 if the preconditioner $\mathbf{M}$ is not nearly singular. We first analyze the properties of the matrix G in (3.3).

Proposition 4.1. *The matrix $G = (g_{ij})_{i,j=1}^M$ in (3.3) is an $M \times M$ complex symmetric Toeplitz matrix. Moreover, the imaginary part $\Im(G)$ of G is a symmetric positive definite Toeplitz matrix.*

Proof. The first statement is obvious. Let $v = [v_1, v_2, \ldots, v_M]^{\mathrm{T}} \in \mathbb{C}^M$, $v \neq 0$ and $v^* = [\bar{v}_1, \bar{v}_2, \ldots, \bar{v}_M]$ denote its complex conjugate. It follows from

$$J_1(z) = \frac{z}{\pi} \int_{-1}^{1} \sqrt{1 - t^2} \exp(\mathrm{i}zt) dt$$

that

$$\begin{aligned}
v^* \Im(G) v &= \sum_{i=1}^{M} \sum_{j=1}^{M} g_{ij}^{\mathrm{im}} \bar{v}_i v_j \\
&= \frac{k_0^2 h_x}{2\pi} \int_{-1}^{1} \sqrt{1 - t^2} \sum_{i=1}^{M} \sum_{j=1}^{M} \exp(\mathrm{i}k_0 h_x |i - j| t) \bar{v}_i v_j dt \\
&= \frac{k_0^2 h_x}{2\pi} \int_{0}^{1} \sqrt{1 - t^2} \sum_{i=1}^{M} \sum_{j=1}^{M} \left(\exp(\mathrm{i}k_0 h_x (i - j) t) + \exp(-\mathrm{i}k_0 h_x (i - j) t)\right) \bar{v}_i v_j dt \\
&= \frac{k_0^2 h_x}{2\pi} \int_{0}^{1} \sqrt{1 - t^2} \left(\left| \sum_{i=1}^{M} \exp(-\mathrm{i}k_0 h_x i t) v_i \right|^2 + \left| \sum_{i=1}^{M} \exp(\mathrm{i}k_0 h_x j t) v_j \right|^2 \right) dt \\
&> 0.
\end{aligned}$$

Therefore, $\Im(G)$ is symmetric and positive definite. □

Remark 4.2. Numerical results show that the real part $\Re(G)$ of G is negative definite; however, no theoretical proof is available.

Remark 4.3. For large arguments $z \gg \frac{3}{4}$, we have [22, Chapter 11]:

$$Y_1(z) \sim \sqrt{\frac{2}{\pi z}} \sin\left(z - \frac{3}{4}\pi\right), \qquad J_1(z) \sim \sqrt{\frac{2}{\pi z}} \cos\left(x - \frac{3}{4}\pi\right).$$

Therefore, if $k_0 h_x |i-j| \gg \frac{3}{4}$, then

$$g_{ij}^{\mathrm{re}} \sim \frac{1}{h_x} \ln\left(1 - \frac{1}{|i-j|^2}\right) \sqrt{\frac{k_0 h_x |i-j|}{2\pi}} \sin\left(k_0 h_x |i-j| - \frac{3}{4}\pi\right),$$
$$g_{ij}^{\mathrm{im}} \sim \frac{1}{h_x} \frac{1}{|i-j|^2} \sqrt{\frac{k_0 h_x |i-j|}{2\pi}} \cos\left(k_0 h_x |i-j| - \frac{3}{4}\pi\right).$$

If we further assume that h_y/h_x and $k_0 h_x$ are constants, we have $h_y |g_{ij}| \sim \mathcal{O}(|i-j|^{-3/2})$ as $|i-j| \to +\infty$. Hence, it is easy to show that the generating function [10] of the Toeplitz matrix $h_y G$ belongs to the Wiener class [10].

We now discuss a property of eigenvalues of a complex symmetric matrix. Let λ be an eigenvalue of a complex symmetric matrix $\mathbf{C} = \mathbf{S} + \mathrm{i}\mathbf{T}$ with $\mathbf{C} = \mathbf{C}^{\mathrm{T}} \in \mathbb{C}^{n\times n}$, $\mathbf{S} = \mathbf{S}^{\mathrm{T}} \in \mathbb{R}^{n\times n}$ and $\mathbf{T} = \mathbf{T}^{\mathrm{T}} \in \mathbb{R}^{n\times n}$. Suppose the eigenvector corresponding to λ is $\mathbf{w} = \mathbf{p} + \mathrm{i}\mathbf{q}$ with $\mathbf{w} \in \mathbb{C}^n$ and $\mathbf{p}, \mathbf{q} \in \mathbb{R}^n$, i.e.,

$$\mathbf{C}\mathbf{w} = \lambda \mathbf{w}.$$

Let $\mathbf{w}^*$ denote the conjugate transpose of $\mathbf{w}$. Then,

$$\begin{aligned}
\lambda \mathbf{w}^*\mathbf{w} &= \mathbf{w}^*\mathbf{C}\mathbf{w} \\
&= (\mathbf{p}^{\mathrm{T}} - \mathrm{i}\mathbf{q}^{\mathrm{T}})(\mathbf{S} + \mathrm{i}\mathbf{T})(\mathbf{p} + \mathrm{i}\mathbf{q}) \\
&= \mathbf{p}^{\mathrm{T}}\mathbf{S}\mathbf{p} + \mathbf{q}^{\mathrm{T}}\mathbf{S}\mathbf{q} + \mathbf{q}^{\mathrm{T}}\mathbf{T}\mathbf{p} - \mathbf{p}^{\mathrm{T}}\mathbf{T}\mathbf{q} + \mathrm{i}(\mathbf{p}^{\mathrm{T}}\mathbf{T}\mathbf{p} + \mathbf{q}^{\mathrm{T}}\mathbf{T}\mathbf{q} + \mathbf{p}^{\mathrm{T}}\mathbf{S}\mathbf{q} - \mathbf{q}^{\mathrm{T}}\mathbf{S}\mathbf{p}) \\
&= \mathbf{p}^{\mathrm{T}}\mathbf{S}\mathbf{p} + \mathbf{q}^{\mathrm{T}}\mathbf{S}\mathbf{q} + \mathrm{i}(\mathbf{p}^{\mathrm{T}}\mathbf{T}\mathbf{p} + \mathbf{q}^{\mathrm{T}}\mathbf{T}\mathbf{q}),
\end{aligned}$$

which leads to

$$\Re(\lambda) = \frac{\mathbf{p}^{\mathrm{T}}\mathbf{S}\mathbf{p} + \mathbf{q}^{\mathrm{T}}\mathbf{S}\mathbf{q}}{\mathbf{w}^*\mathbf{w}}, \qquad \Im(\lambda) = \frac{\mathbf{p}^{\mathrm{T}}\mathbf{T}\mathbf{p} + \mathbf{q}^{\mathrm{T}}\mathbf{T}\mathbf{q}}{\mathbf{w}^*\mathbf{w}}.$$

Therefore, if $\mathbf{S}$ and $\mathbf{T}$ are positive (negative) definite, then $\Re(\lambda) > 0 (< 0)$ and $\Im(\lambda) > 0 (< 0)$.

Note that E in (3.8) is a real diagonal matrix. It follows from Proposition 4.1, Theorem A.1 and the discussion above that the matrices $\mathbf{A}$ and $\mathbf{M}$ are nonsingular. We have

$$\mathbf{A}\mathbf{M}^{-1} = I_M + (\mathbf{A} - \mathbf{M})\mathbf{M}^{-1} = I_M + S_M(s(h_y G) - h_y G) S_M \mathbf{M}^{-1}.$$

On the basis of Proposition 4.1, Remarks 4.2 and 4.3, and the arguments in [10], we know that $\|s(h_y G) - h_y G\| \to 0$ as $M \to +\infty$. Therefore, the spectrum of $\mathbf{A}\mathbf{M}^{-1}$ is clustered around 1 if the preconditioner $\mathbf{M}$ is not nearly singular.

5. Numerical results

In this section we report numerical results for a cavity with two different media. We refer the reader to [23–31] for other discretization schemes and more numerical experiments. The implementations of Algorithm I are done in FORTRAN on a computer with a 2.26 GHz CPU. The P-COCG solver is used for the interface system (3.8). Both the preconditioner $\mathbf{P}$ (3.9) and the preconditioner $\mathbf{M}$ (3.10) are evaluated. The zero vector is used as the initial guess. The iteration is terminated at the mth iteration if the residual satisfies

$$\frac{\|r_m\|}{\|\check{g}\|} \le 10^{-5}.$$

Let the cavity of interest be the box $\Omega = [0, 1] \times [-1, 0]$. All the cases considered here are source free. We use a uniform grid with $M = N$. The physical parameter of interest is the RCS, which is defined by

$$\sigma(\phi) = \frac{4}{k_0} |P(\phi)|^2$$

where ϕ is the observation angle and $P(\phi)$ is the far-field coefficient given by

$$P(\phi) = \frac{k_0}{2} \sin\phi \int_{\Gamma} u \exp(\mathrm{i}k_0 x \cos\phi) dx.$$

When the incident and observation directions are the same, we have the backscatter RCS:

$$\text{Backscatter RCS}(\phi) = 10 \log_{10} \sigma(\phi) \text{ dB}.$$

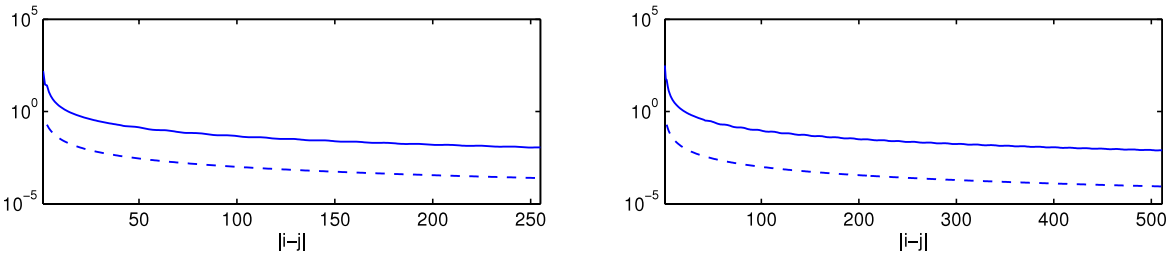

Fig. 2. The magnitude of the first column of G. The solid line denotes $|g_{ij}|$ and the dashed line denotes $|i-j|^{-3/2}$. Left: $k_0 = 16\pi$. Right: $k_0 = 32\pi$.

Table 1
Number of iterations and CPU time in seconds (in parentheses) required by P-COCG for the interface system (3.8) for the cavity with the homogeneous medium $\varepsilon_r = 1$. All results are obtained at normal incidence.

k_0	$M \times N$	Preconditioner **P**	Preconditioner **M**
$k_0 = 4\pi$	1023×1023	7 (1.5625E-02)	5 (1.5625E-02)
	2047×2047	7 (4.6875E-02)	6 (3.1250E-02)
$k_0 = 8\pi$	1023×1023	10 (3.1250E-02)	5 (1.5625E-02)
	2047×2047	10 (6.2500E-02)	5 (3.1250E-02)
$k_0 = 16\pi$	1023×1023	19 (6.2500E-02)	5 (1.5625E-02)
	2047×2047	21 (1.2500E-01)	5 (3.1250E-02)
$k_0 = 32\pi$	1023×1023	20 (6.2500E-02)	5 (1.5625E-02)
	2047×2047	24 (1.2500E-01)	5 (3.1250E-02)

Consider the cavity with two different media:

- Homogeneous.

$$\varepsilon_r(x, y) = 1.$$

- Non-homogeneous.

$$\varepsilon_r(x, y) = \begin{cases} 1, & y \geq -\dfrac{1}{3}, \\ 2, & y < -\dfrac{2}{3}, \\ \dfrac{3}{2} & \text{otherwise.} \end{cases} \tag{5.1}$$

Obviously, both media are layered.

We present the absolute values of the entries in the first column of the matrix G in Fig. 2. Here, 32 points per wavelength are used. It is clear that the $|g_{ij}|$ decays like $\mathcal{O}(|i-j|^{-3/2})$.

The eigenvalue distributions of the matrix $\mathbf{A}$ and $\mathbf{A}\mathbf{M}^{-1}$ for the cavity with the two media with respect to different wavenumbers are given in Figs. 3 and 4. Here, 32 points per wavelength are used. We observe that there are some eigenvalues with negative real parts in all cases. As a comparison, the eigenvalues of the preconditioned matrix $\mathbf{A}\mathbf{M}^{-1}$ are located in the right half-plane with real parts larger than 0.75 and clustered around 1, which is in good agreement with our analysis in Section 4. Many Krylov subspace iterative algorithms have good convergence behavior for such a linear system; see, for example, the discussion in [32, section].

The real parts of the electric fields for the two media with $k_0 = 16\pi, 32\pi$ are given in Figs. 5 and 6. The magnitude of the electric fields on the aperture of the cavity and the backscatter RCS for the two media with $k_0 = 16\pi, 32\pi$ are given in Figs. 7 and 8. Here, 32 points per wavelength are used. The highly oscillatory nature of the fields for large wavenumbers is observed.

The CPU time and the number of iterations of P-COCG for the interface system (3.8) are shown in Tables 1 and 2. Clearly,

(I) the number of iterations of P-COCG with the preconditioner **P** is almost independent of the mesh size and increases as the wavenumber k_0 increases;
(II) the number of iterations of P-COCG with the preconditioner **M** is independent of the mesh size and the wavenumber k_0.

For large wavenumber problems, about 75% of the CPU time is saved.

6. Concluding remarks

In this paper, using the optimal sine transform based approximation we have proposed a new preconditioner for the interface system arising in the fast algorithm for the electromagnetic scattering from a large cavity with layered media.

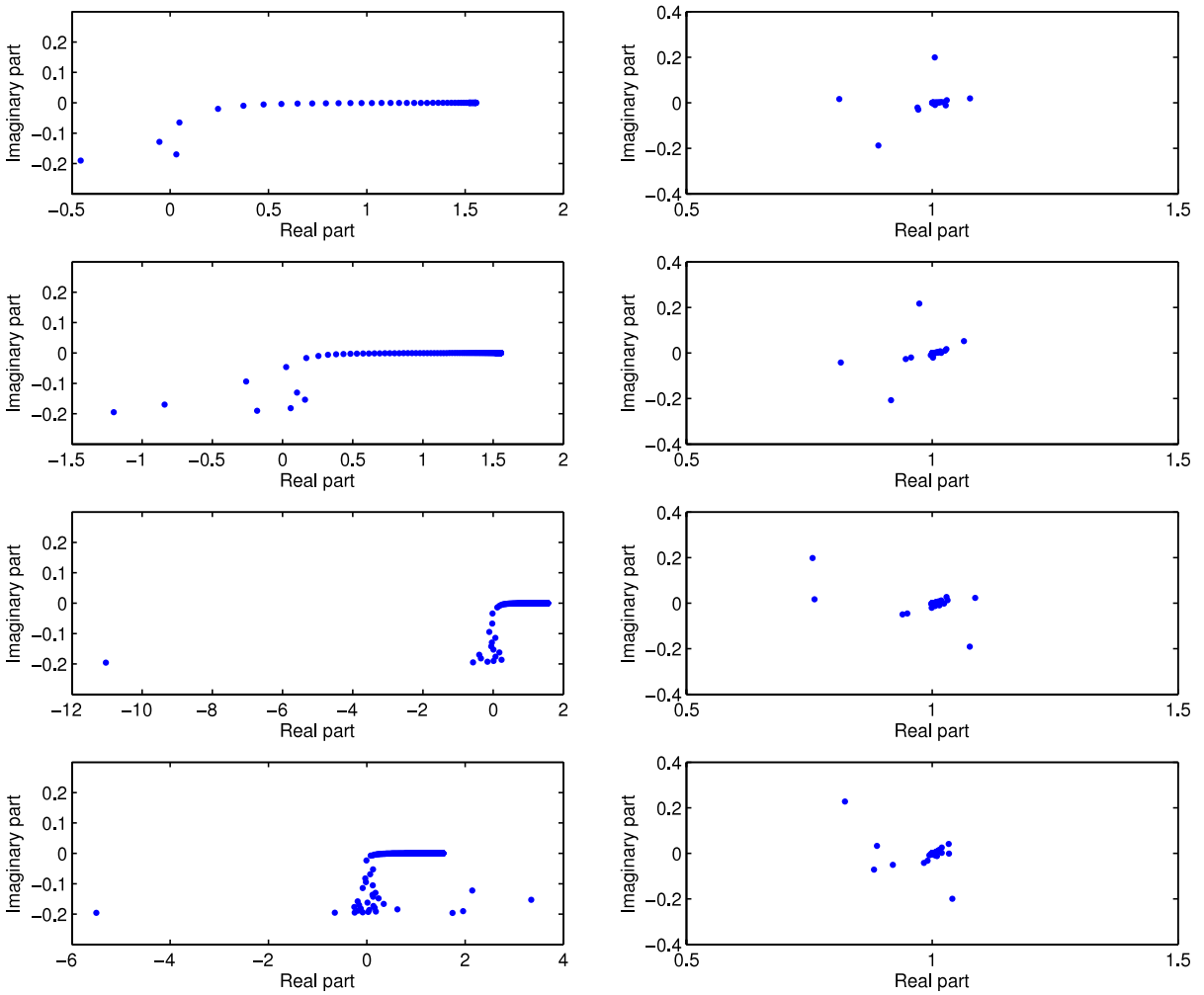

Fig. 3. The eigenvalue distributions of **A** (left) and the preconditioned matrix $\mathbf{AM}^{-1}$ (right) for the cavity with the homogeneous medium $\varepsilon_r = 1$; from top to bottom: $k_0 = 4\pi, 8\pi, 16\pi, 32\pi$.

Table 2
Number of iterations and CPU time in seconds (in parentheses) required by P-COCG for the interface system (3.8) for the cavity with non-homogeneous medium (5.1). All results are obtained at normal incidence.

k_0	$M \times N$	Preconditioner **P**	Preconditioner **M**
$k_0 = 4\pi$	1023 × 1023	6 (1.5625E-02)	5 (1.5625E-02)
	2047 × 2047	6 (3.1250E-02)	5 (3.1250E-02)
$k_0 = 8\pi$	1023 × 1023	10 (3.1250E-02)	5 (1.5625E-02)
	2047 × 2047	11 (6.2500E-02)	5 (3.1250E-02)
$k_0 = 16\pi$	1023 × 1023	14 (3.1250E-02)	5 (1.5625E-02)
	2047 × 2047	14 (7.8125E-02)	5 (3.1250E-02)
$k_0 = 32\pi$	1023 × 1023	30 (7.8125E-02)	5 (1.5625E-02)
	2047 × 2047	30 (1.5625E-01)	5 (3.1250E-02)

Theoretical analysis shows that the spectrum of the preconditioned matrix is clustered around 1 if the preconditioner is not nearly singular. Numerical results show that the number of iterations of the P-COCG solver combined with this preconditioner is independent of the mesh size and the wavenumber. The extension to the transverse electric polarization (in which the Dirichlet boundary conditions are replaced by the Neumann boundary conditions, and the hyper-singular integral boundary condition (2.2)(c) is replaced by a weakly singular integral boundary condition [25] in comparison with the transverse magnetic polarization case) is straightforward. The only essential change is the replacement of the optimal sine transform based approximation by the optimal cosine transform based approximation [33–35].

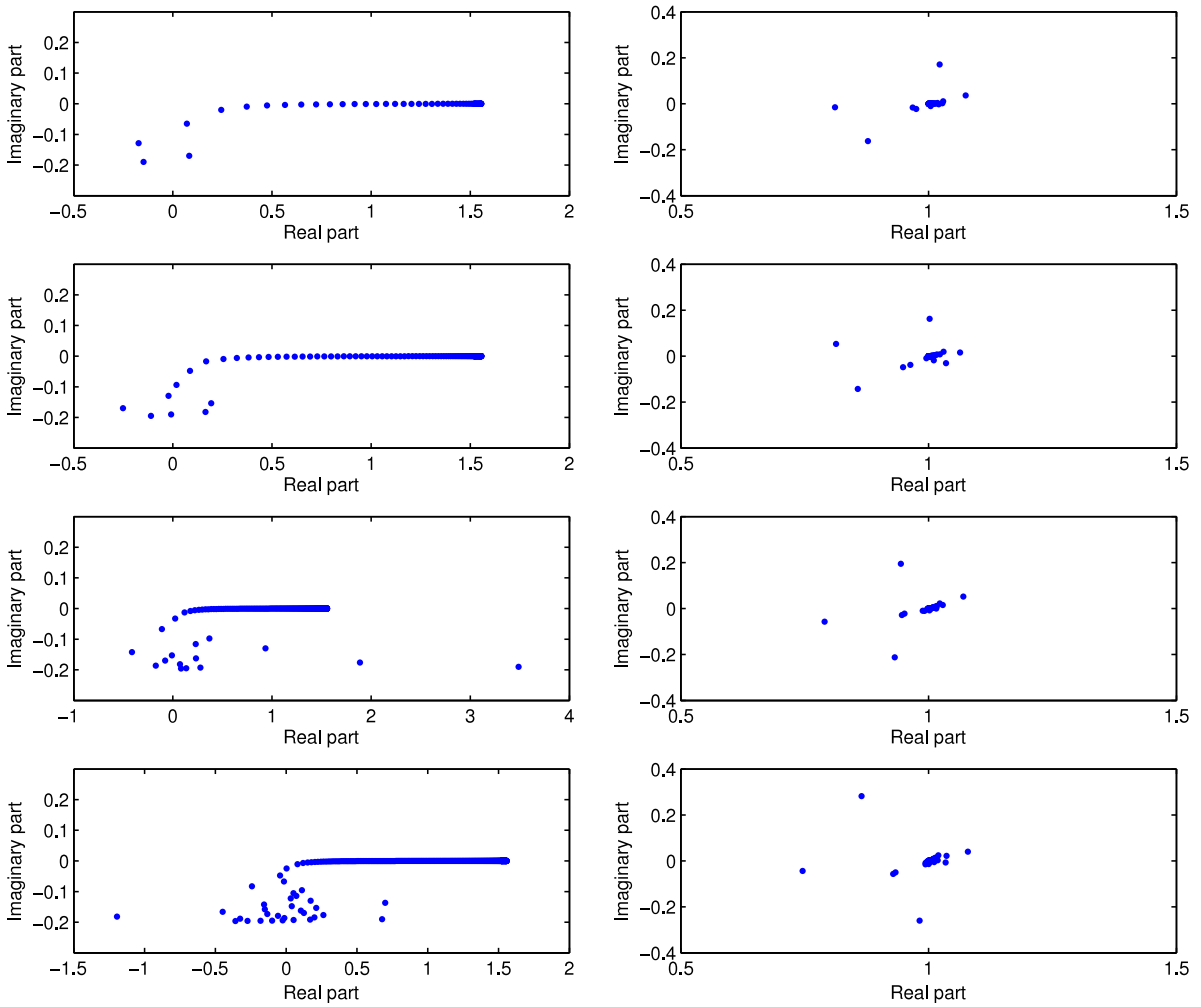

Fig. 4. The eigenvalue distributions of $\mathbf{A}$ (left) and the preconditioned matrix $\mathbf{AM}^{-1}$ (right) for the cavity with the non-homogeneous medium (5.1); from top to bottom: $k_0 = 4\pi, 8\pi, 16\pi, 32\pi$.

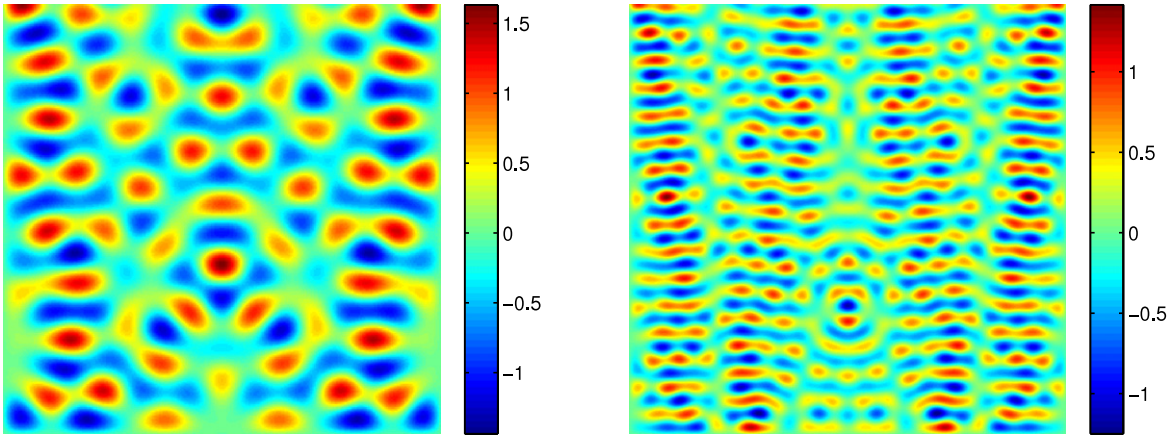

Fig. 5. Real parts of the electric fields (normal incidence) for the cavity with the homogeneous medium $\varepsilon_r = 1$. Left: $k_0 = 16\pi$. Right: $k_0 = 32\pi$.

We point out that the optimal sine transform based approximation together with the layered medium model can be used as a preconditioning technique for the cavity problem with general medium. In [31] we have proposed a composite preconditioner, which employs the matrix decomposition algorithms (see, for example, [36,37]).

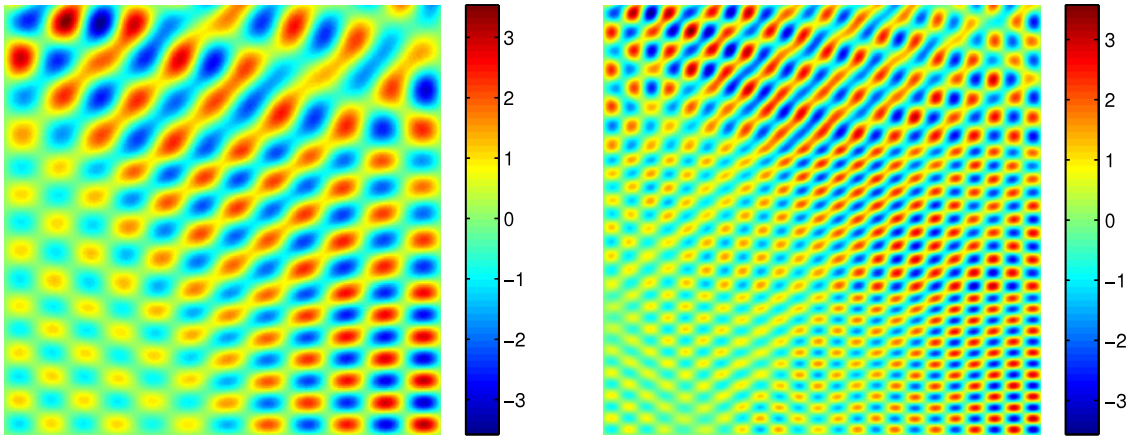

Fig. 6. Real parts of the electric fields (incident angle $\theta = \pi/4$) for the cavity with the non-homogeneous medium (5.1). Left: $k_0 = 16\pi$. Right: $k_0 = 32\pi$.

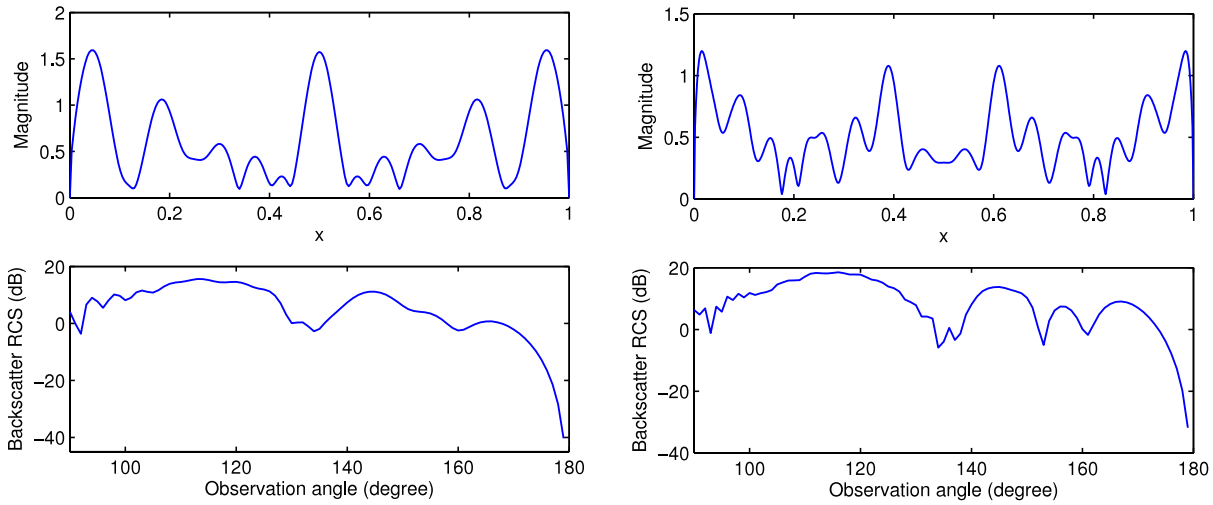

Fig. 7. The magnitude of the electric field (normal incidence) on the aperture of the cavity and the backscatter RCS for the cavity with the homogeneous medium $\varepsilon_r = 1$. Left: $k_0 = 16\pi$. Right: $k_0 = 32\pi$.

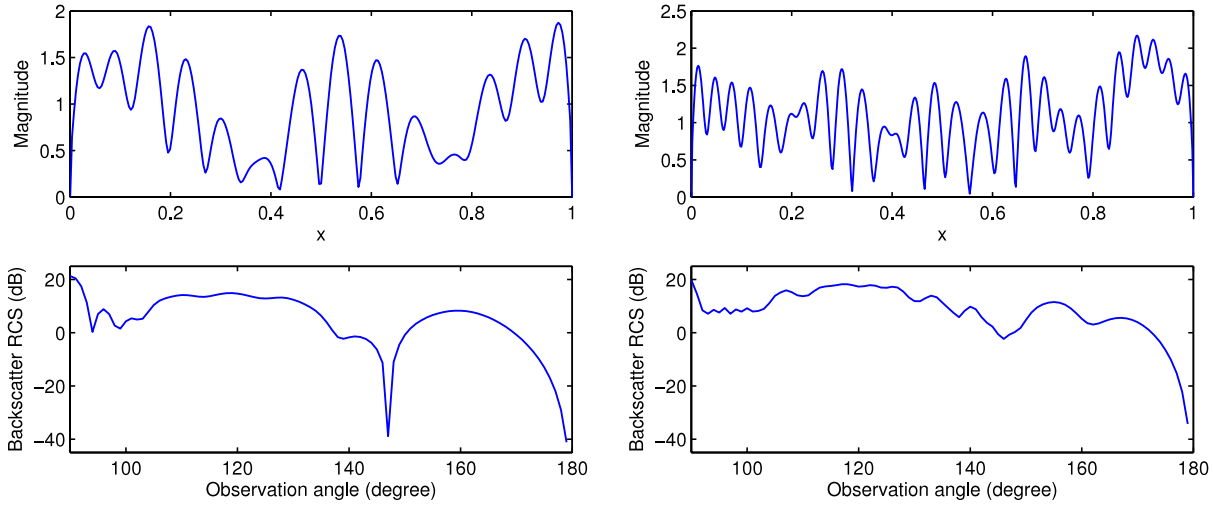

Fig. 8. The magnitude of the electric field (incident angle $\theta = \pi/4$) on the aperture of the cavity and the backscatter RCS for the cavity with the non-homogeneous medium (5.1). Left: $k_0 = 16\pi$. Right: $k_0 = 32\pi$.

Acknowledgments

The author thanks his Ph.D. supervisor Prof. Weiwei Sun for fruitful discussions on this work. The author also thanks the two anonymous reviewers for helpful comments that improved the presentation of this work.

The research of the author was partially supported by a grant from the Research Grants Council of the Hong Kong Special Administrative Region, China (Project No. CityU 103410), the Academy of Finland grant 128474 and the Väisälä Foundation of the Finnish Academy of Science and Letters.

Appendix A. Optimal sine transform based approximations

Denote the discrete sine transformation matrix by

$$S_n = \left[\sqrt{\frac{2}{n+1}}\left(\sin\frac{ij\pi}{n+1}\right)\right]_{i,j=1}^{n}.$$

We have $S_n S_n^{\mathrm{T}} = S_n^2 = I_n$. The matrix–vector product $S_n v$ can be obtained in $\mathcal{O}(n\log n)$ operations for any n-vector v. Let A be an $n \times n$ matrix. The optimal sine transform based approximation $s(A)$ is defined to be the minimizer of $\|P - A\|_{\mathrm{F}}$ over the set of matrices P that can be diagonalized by S_n, where $\|\cdot\|_{\mathrm{F}}$ denotes the Frobenius norm. We have the following theorem.

Theorem A.1 (*[10, Theorem 2]*)**.** *Let A be an n-by-n real symmetric matrix. Let $s(\cdot)$ denote the optimal sine transform based approximation. Then $s(A)$ is real symmetric. Moreover, we have*

$$\lambda_{\min}(A) \le \lambda_{\min}(s(A)) \le \lambda_{\max}(s(A)) \le \lambda_{\max}(A),$$

where $\lambda_{\max}(\cdot)$ and $\lambda_{\min}(\cdot)$ denote the largest and the smallest eigenvalues respectively.

Let $P = S_n \Lambda_s S_n$, $e_1 = [1, 0, \ldots, 0]^{\mathrm{T}}$ and $e = [1, 1, \ldots, 1]^{\mathrm{T}}$; then we have

$$D_s^{-1} S_n P e_1 = \Lambda_s e, \tag{A.1}$$

where D_s is the diagonal matrix with diagonal $S_n e_1$. Thus, to compute the eigenvalues of P, we only need the first column of P. For a diagonal matrix or a Toeplitz matrix, $s(A)$ can be obtained in $\mathcal{O}(n)$ operations. See Chapter 5 of [35] for details. Next, we list the formulas [38] for computing $s(A)$ when A is a symmetric Toeplitz matrix.

Let T_n be an $n \times n$ symmetric Toeplitz matrix:

$$T_n = \begin{bmatrix} t_0 & t_1 & \cdots & t_{n-2} & t_{n-1} \\ t_1 & t_0 & t_1 & \cdots & t_{n-2} \\ \vdots & t_1 & t_0 & \ddots & \vdots \\ t_{n-2} & \cdots & \ddots & \ddots & t_1 \\ t_{n-1} & t_{n-2} & \cdots & t_1 & t_0 \end{bmatrix}.$$

Let $s = [s_1, s_2, \ldots, s_n]^{\mathrm{T}}$ be the first column of $s(T_n)$. The explicit formula for s is given below:

$$s_j = \begin{cases} t_0 - \left(\dfrac{n-2}{n+1}\right) t_2, & j = 1, \\ t_1 - \left(\dfrac{n-3}{n+1}\right) t_3, & j = 2, \\ \left(\dfrac{n-j+3}{n+1}\right) t_{j-1} - \left(\dfrac{n-j-1}{n+1}\right) t_{j+1}, & j = 3, 4, \ldots, n-2, \\ \left(\dfrac{4}{n+1}\right) t_{n-2}, & j = n-1, \\ \left(\dfrac{3}{n+1}\right) t_{n-1}, & j = n. \end{cases} \tag{A.2}$$

Appendix B. Preconditioned COCG

Let $\mathbf{A}$ and $\mathbf{M}$ be complex symmetric. We present the details of the preconditioned COCG (P-COCG) solver as follows.

Algorithm P-COCG: $\mathbf{A}\mathbf{M}^{-1}\mathbf{z} = \mathbf{b}$, $\mathbf{x} = \mathbf{M}^{-1}\mathbf{z}$

Choose $\mathbf{x}_0$;
set $\mathbf{r}_0 = \mathbf{b} - \mathbf{A}\mathbf{x}_0$ and $\mathbf{p}_0 = \mathbf{M}^{-1}\mathbf{r}_0$;
for $k = 0, 1, 2, \ldots$, do until convergence or breakdown:
$\mathbf{x}_{k+1} = \mathbf{x}_k + \alpha_k \mathbf{p}_k$;
$\mathbf{r}_{k+1} = \mathbf{r}_k - \alpha_k \mathbf{A}\mathbf{p}_k$;
$\mathbf{p}_{k+1} = \mathbf{M}^{-1}\mathbf{r}_{k+1} + \beta_k \mathbf{p}_k$;
where
$$\alpha_k = \frac{\mathbf{r}_k^{\mathrm{T}}\mathbf{M}^{-1}\mathbf{r}_k}{\mathbf{p}_k^{\mathrm{T}}\mathbf{A}\mathbf{p}_k};\ \beta_k = \frac{\mathbf{r}_{k+1}^{\mathrm{T}}\mathbf{M}^{-1}\mathbf{r}_{k+1}}{\mathbf{r}_k^{\mathrm{T}}\mathbf{M}^{-1}\mathbf{r}_k}.$$

The main computational cost and storage for P-COCG consist of one matrix–vector product, $\mathbf{A}\mathbf{p}_k$, and one preconditioner solve, $\mathbf{M}^{-1}\mathbf{r}_{k+1}$, per iteration and five length n vectors, $\mathbf{b}$, $\mathbf{x}_{k+1}$, $\mathbf{r}_{k+1}$, $\mathbf{p}_{k+1}$, one slack vector for $\mathbf{A}\mathbf{p}_k$ and $\mathbf{M}^{-1}\mathbf{r}_{k+1}$. The preconditioner $\mathbf{M}$ in P-COCG also has to be complex symmetric. The derivation of P-COCG is similar to that of the preconditioned conjugate gradient (P-CG) method in [13, Section 5.2], which uses the inner product $\mathbf{x}^*\mathbf{M}\mathbf{y}$ for the left preconditioning case $\mathbf{M}^{-1}\mathbf{A}\mathbf{x} = \mathbf{M}^{-1}\mathbf{b}$ with Hermitian and positive definite matrices $\mathbf{A}$ and $\mathbf{M}$. The only essential change of P-COCG with respect to P-CG is the replacement of the inner product $\mathbf{x}^*\mathbf{M}\mathbf{y}$ by the bilinear form $\mathbf{x}^{\mathrm{T}}\mathbf{M}^{-1}\mathbf{y}$.

The P-COCG algorithm may suffer from two kinds of breakdowns. The first kind of breakdown occurs if $\mathbf{p}_k^{\mathrm{T}}\mathbf{A}\mathbf{p}_k = 0$. This type of breakdown is uncured. The second kind of breakdown is related to the quasi-null-space formed in the algorithm. The quasi-null-space is characterized by the situation that for $\mathbf{r}_k \neq 0$, $\mathbf{r}_k^{\mathrm{T}}\mathbf{r}_k = 0$. This kind of breakdown can be overcome by a look-ahead strategy [39, Chapter 7] as has been suggested for the bi-conjugate gradient method [40], by restarting the process or by switching to another algorithm.

References

[1] H.T. Anastassiu, A review of electromagnetic scattering analysis for inlets, cavities, and open ducts, IEEE Antennas Propag. Mag. 45 (2003) 27–40.
[2] F.G. Hu, C.F. Wang, Preconditioned formulation of FE–BI equations with domain decomposition method for calculation of electromagnetic scattering from cavities, IEEE Trans. Antennas Propag. 57 (2009) 2506–2511.
[3] J. Huang, A.W. Wood, Numerical simulation of electromagnetic scattering induced by an overfilled cavity in the ground plane, IEEE Antennas Wirel. Propag. Lett. 4 (2005) 224–228.
[4] J.M. Jin, The Finite Element Method in Electromagnetics, second ed., Wiley-Interscience, John Wiley & Sons, New York, 2002.
[5] J.M. Jin, J. Liu, Z. Lou, C.S.T. Liang, A fully high-order finite-element simulation of scattering by deep cavities, IEEE Trans. Antennas Propag. 51 (2003) 2420–2429.
[6] J. Liu, J.M. Jin, A special higher order finite-element method for scattering by deep cavities, IEEE Trans. Antennas Propag. 48 (2000) 694–703.
[7] W.D. Wood Jr., A.W. Wood, Development and numerical solution of integral equations for electromagnetic scattering from a trough in a ground plane, IEEE Trans. Antennas Propag. 47 (1999) 1318–1322.
[8] G. Bao, W. Sun, A fast algorithm for the electromagnetic scattering from a large cavity, SIAM J. Sci. Comput. 27 (2005) 553–574 (electronic).
[9] P. Swarztrauber, FFTPACK, NCAR Boulder CO 1985, Also available from netlibornl.gov.
[10] R.H. Chan, M.K. Ng, C.K. Wong, Sine transform based preconditioners for symmetric Toeplitz systems, Linear Algebra Appl. 232 (1996) 237–259.
[11] D.A.H. Jacobs, The exploitation of sparsity by iterative methods, in: I.S. Duff (Ed.), Sparse Matrices and their Uses, Springer, 1981, pp. 191–222.
[12] H.A. van der Vorst, J.B.M. Melissen, A Petrov–Galerkin type method for solving $Ax = b$, where A is symmetric complex, IEEE Trans. Magn. 26 (1990) 706–708.
[13] H.A. van der Vorst, Iterative Krylov Methods for Large Linear Systems, in: Cambridge Monographs on Applied and Computational Mathematics, vol. 13, Cambridge University Press, Cambridge, 2003.
[14] H. Ammari, G. Bao, A.W. Wood, Analysis of the electromagnetic scattering from a cavity, Japan J. Indust. Appl. Math. 19 (2002) 301–310.
[15] M. Abramowitz, I.A. Stegun (Eds.), Handbook of Mathematical Functions with Formulas, Graphs, and Mathematical Tables, Dover Publications Inc., New York, 1992, Reprint of the 1972 edition.
[16] J. Wu, Y. Wang, W. Li, W. Sun, Toeplitz-type approximations to the Hadamard integral operator and their applications to electromagnetic cavity problems, Appl. Numer. Math. 58 (2008) 101–121.
[17] F. Di Benedetto, Iterative solution of Toeplitz systems by preconditioning with the discrete sine transform, in: Proc. SPIE Conference in Advanced Signal Processing Algorithms, Architectures, and Implementations, Citeseer.
[18] T. Huckle, Iterative methods for ill-conditioned Toeplitz matrices, Calcolo 33 (1996) 177–190, Toeplitz matrices: structures, algorithms and applications, Cortona, 1996.
[19] R.H. Chan, C.K. Wong, Sine transform based preconditioners for elliptic problems, Numer. Linear Algebra Appl. 4 (1997) 351–368.
[20] F. Di Benedetto, Preconditioning of block Toeplitz matrices by sine transforms, SIAM J. Sci. Comput. 18 (1997) 499–515.
[21] F. Di Benedetto, Solution of Toeplitz normal equations by sine transform based preconditioning, Linear Algebra Appl. 285 (1998) 229–255.
[22] G.B. Arfken, H.J. Weber, Mathematical Methods for Physicists, sixth ed., Harcourt, Academic Press, Burlington, MA, 2005.
[23] Y. Wang, K. Du, W. Sun, Fast algorithms for the electromagnetic scattering from rectangular cavities, in: Recent Advances in Computational Mathematics, Int. Press, Boston, MA, 2008, pp. 13–38.
[24] Y. Wang, K. Du, W. Sun, A second-order method for the electromagnetic scattering from a large cavity, Numer. Math. Theory Methods Appl. 1 (2008) 357–382.
[25] K. Du, Numerical computation of electromagnetic scattering from large cavities, Ph.D. Thesis, City University of Hong Kong, 2009.
[26] Y. Wang, K. Du, W. Sun, Preconditioning iterative algorithm for the electromagnetic scattering from a large cavity, Numer. Linear Algebra Appl. 16 (2009) 345–363.
[27] K. Du, On initial guesses of preconditioned Krylov subspace methods on sparse subspaces, Manuscript, 2010.
[28] K. Du, Two transparent boundary conditions for electromagnetic scattering from two-dimensional overfilled cavities, J. Comput. Phys. 230 (2011) 5822–5835.

[29] K. Du, W. Sun, Electromagnetic scattering from a large partly covered cavity, J. Comput. Appl. Math. 235 (2011) 3791–3806.
[30] K. Du, GMRES with adaptively deflated restarting and its performance on an electromagnetic cavity problem, Appl. Numer. Math. 61 (2011) 977–988.
[31] K. Du, A composite preconditioner for the electromagnetic scattering from a large cavity, J. Comput. Phys. 230 (2011) 8089–8108.
[32] M. Benzi, D. Bertaccini, Block preconditioning of real-valued iterative algorithms for complex linear systems, IMA J. Numer. Anal. 28 (2008) 598–618.
[33] R.H. Chan, T.F. Chan, C.K. Wong, Cosine transform based preconditioners for total variation deblurring, IEEE Trans. Image Process. 8 (1999) 1472–1478.
[34] M.K. Ng, R.H. Chan, T.F. Chan, A.M. Yip, Cosine transform preconditioners for high resolution image reconstruction, Linear Algebra Appl. 316 (2000) 89–104, Conference Celebrating the 60th Birthday of Robert J. Plemmons, Winston-Salem, NC, 1999.
[35] M.K. Ng, Iterative methods for Toeplitz systems, in: Numerical Mathematics and Scientific Computation, Oxford University Press, New York, 2004.
[36] K. Du, G. Fairweather, Q.N. Nguyen, W. Sun, Matrix decomposition algorithms for the C^0-quadratic finite element Galerkin method, BIT 49 (2009) 509–526.
[37] G. Fairweather, A. Karageorghis, J. Maack, Compact optimal quadratic spline collocation methods for the Helmholtz equation, J. Comput. Phys. 230 (2011) 2880–2895.
[38] R.H. Chan, M.K. Ng, Conjugate gradient methods for Toeplitz systems, SIAM Rev. 38 (1996) 427–482.
[39] Y. Saad, Iterative Methods for Sparse Linear Systems, second ed., Society for Industrial and Applied Mathematics, Philadelphia, PA, 2003.
[40] R. Fletcher, Conjugate gradient methods for indefinite systems, in: Numerical Analysis (Proc. 6th Biennial Dundee Conf., Univ. Dundee, Dundee, 1975), in: Lecture Notes in Math., vol. 506, Springer, Berlin, 1976, pp. 73–89.